Observation of Electrical, Dielectric and Magneto-dielectric Properties of Terbium Doped Bismuth Ferrite Nanoparticles above Room Temperature

Monalisa Halder[1], Jinia Datta[2], Raja Mallick[3], Ranjita Sinha[4] , Khusi Smriti[5], Chandan Kumar Raul[6], Shubhadip Atta[6] and Ajit Kumar Meikap*

[1]Department of Basic Science and Humanities, Abacus Institute of Engineering and Management, Mogra, Hooghly, India-712148
[2]Principal-in-Charge, Abacus Institute of Engineering and Management, Mogra, Hooghly, India-712148
[3]2nd Year B.Tech. Student, Department of Electronics & Communication Engineering, Abacus Institute of Engineering and Management, Mogra, Hooghly, India-712148
[4]Department of BS&HU (Physics), Asansol Engineering College, Kanyapur, Asansol, India-713305
[5]2nd Year B.Tech. Student, Department of Information Technology, Asansol Engineering College, Kanyapur, Asansol, India-713305
[6]Department of Physics, National Institute of Technology, Durgapur, India-713209
**Corresponding author: monalisahldr18@gmail.com*

Abstract

The effect of rare earth transition metal (Tb) ions doping in A site of bismuth ferrite (BFO) nanoparticles are studied from electrical, dielectric and magneto-dielectric aspects. A detailed study on dielectric properties of the Tb doped bismuth ferrite nanoparticles is done over a wide temperature range in a frequency range of 20 Hz - 2 MHz. Observation on magneto-dielectric response of the sample is done at room temperature upon applying external transverse magnetic field.

Keywords: *Bismuth ferrite, Electrical measurements, Electric modulus spectroscopy, Magneto-dielectric response*

1. Introduction

Perovskite structured bismuth ferrite is a distinctive multiferroic material that has attracted broad interests due to its multifunctionality and potential applications in electronic world. Bismuth ferrite ($BiFeO_3$) exhibits coupled ferroelectric and antiferromagnetic characteristics at room temperature [1]. But due to antiferromagnetic spin ordering, $BiFeO_3$ has zero remnant magnetization which is not desirable in magneto-ferroelectric applications [2]. Enhancement of electrical, magnetic properties has been reported with the doping of other divalent or trivalent ions at A or B site of Bismuth ferrite [3]. Meanwhile, the space charge polarisation induced by the dopants can act as additional dipoles. Doping by rare-earth ion at the Bi site or Fe site can produce ferromagnetism in $BiFeO_3$ material [4-9]. Lazenka et al. discussed the impact of La, Nd and Gd doping of BiFeO3 thin films [1]. Ghosh et al. reported electronic and magnetic properties of La and Sr doped $BiFeO_3$ [10]. Mumtaz et al. reported peculiar magnetism in Eu substituted $BiFeO_3$ and its correlation with local structure [11]. Zhang et al. reported dielectric, ferroelectric and

magnetic properties of Sm doped $BiFeO_3$ ceramics [4]. Rao et al. investigated structural, magnetic and optical properties of Y, Ho and Er substituted $BiFeO_3$[12].

In the present work, we have synthesized rare-earth ion terbium (Tb) doped bismuth ferrite (BFO) nanoparticles (NPs) and studied the morphological, electrical, magnetic effects on doping.

2. Experimental Details

2.1 Material Synthesis

Sol-gel synthesis of terbium (Tb) doped Bismuth ferrite NPs is done using nitrate as precursor materials. For the preparation of $Bi_{0.95}Tb_{0.05}FeO_3$ NPs, weighted amount of $Bi(NO_3)_3.5H_2O$, $Fe(NO_3)_3.9H_2O$, $Tb(NO_3)_3.6H_2O$ are taken to make precursor solution under magnetic stirring. To keep pH level in acidic region, 69% HNO_3 is added to the nitrate solution by two-three drops. All the solutions are mixed up slowly under stirring. Tartaric acid is added drop wise to the solution and the solution changes its colour. The final solution is stirred under high temperature for 2 hours and is kept in oven overnight. The sample is crushed and calcined at 550° C for 2 hours. Finally by grinding the sample, we get the sample.

2.2 Characterisation Techniques

Morphological analysis of Tb doped BFO NPs is done using scanning electron microscope (ZEISS EVO-MA 10) and transmission electron microscope (HRTEM JEOL 2011). To study the charge carrier conduction mechanism of the NPs, metal (silver) electrode contacts are attached on the both side of the pellet of the sample for the formation of a capacitive system. The electrical and dielectric measurements are studied in the frequency window 20 Hz – 2 MHz using Agilent E 4980A precision LCR meter above room temperature. Using an electromagnet (EM-250), magnetodielectric studies of the samples are made with the variation of the external transverse magnetic field ($H \leq 1$ T) at room temperature.

3. Results and Discussions

Fig. 1 shows the FESEM and TEM images of Tb doped BFO nanoparticles. Generally undoped BFONPs are larger may be due to agglomeration which was seen in our previous work [13]. But after Tb doping, the particles are less agglomerating and possess almost uniform hexagonal structure and size. It is clear also from the TEM image also (shown in Fig. 1), the nanoparticles are hexagonal in structure.

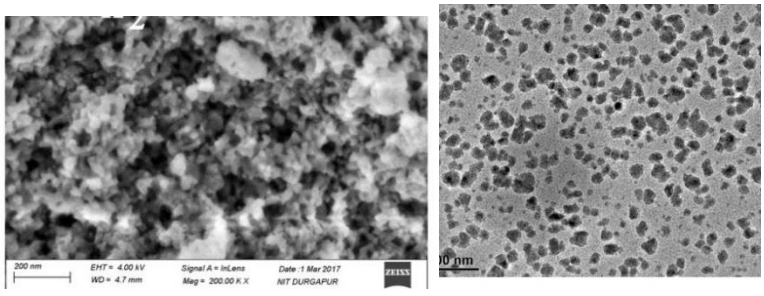

FIG 1.FESEM and TEM images of Tb doped BFO.

Fig. 2 shows the frequency variation of real permittivity [dielectric constant (ε')] of the sample at different temperatures. At lower frequencies, the dielectric constant values are higher due to the electrode polarisation effect. But in higher frequencies, dielectric constant drastically reduces and doesn't get affected by increasing more frequency value. Usually, with the rise in frequency, the dielectric constant drops because the net polarization (i.e. space charge, dipolar, atomic, ionic) of any dielectric material reduces as each polarization mechanism ceases to contribute [14]. The dielectric property enhances upon Tb doping in BFO NPs. The doped samples show a slight decrement in dielectric constant at lower temperatures below 350 K and then show an increase at higher temperature. Similar observation has been studied by Zhang et al. [15].

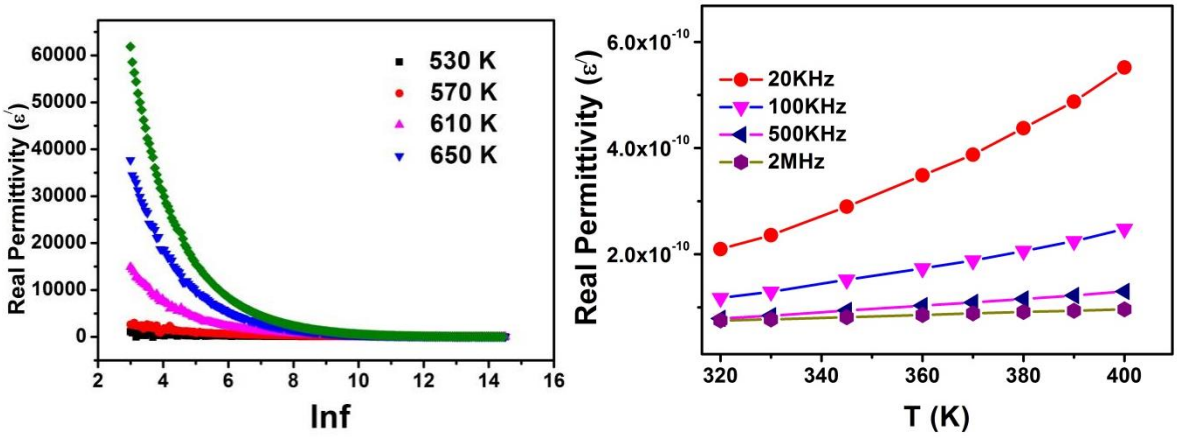

FIG 2. Variation of real permittivity (dielectric constant) of Tb doped BFO NPs with frequency and with temperature respectively

Temperature dependent variation of permittivity is more prominent at lower frequencies than that of higher one. At a particular frequency, the value of the dielectric constant increases thoroughly with temperature. At high frequency, dipoles get opposed in orienting themselves along the applied field. For the mutual movement of dipoles and charges, an electric relaxation arises. The dielectric relaxation behaviour is the result of the combination of two different type of polarisation mechanisms (interfacial polarisation and space charge polarisation) related to the physical movement of the charges and the relaxation time required for the displacement [16].

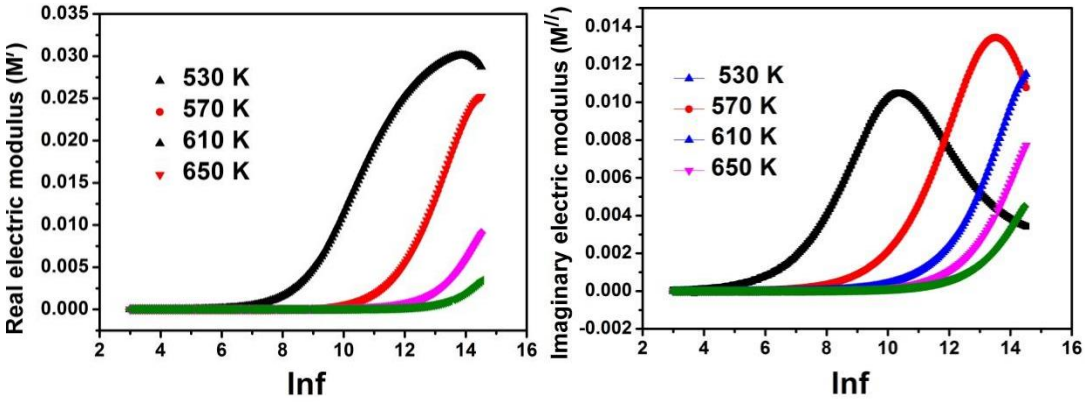

FIG 3. Frequency variation of real and imaginary electric modulus of Tb doped BFO NPs

Fig. 3 shows the frequency variation of the real part and imaginary part of electric modulus (M') of Tb doped BFO NPs at different temperatures. M' continuously increases with a trend to saturate at a maximum asymptotic value for each sample. The behaviour suggests the dominant contribution of the short range mobility of charge carriers in conduction process [17]. In lower frequencies, the lower values of M' implies the conduction phenomena due to the negligible contribution of the electrode polarisation as well as long range mobility of charge carriers of the material. The frequency variation of imaginary part (M'') of electric modulus spectra plots of the sample show the existence of relaxation peak. The relaxation peak moves to the higher frequency as the temperature increases. The observed asymmetric nature of the peaks suggests the spread of relaxation time supported by the non-Debye type of relaxation in the sample [18].

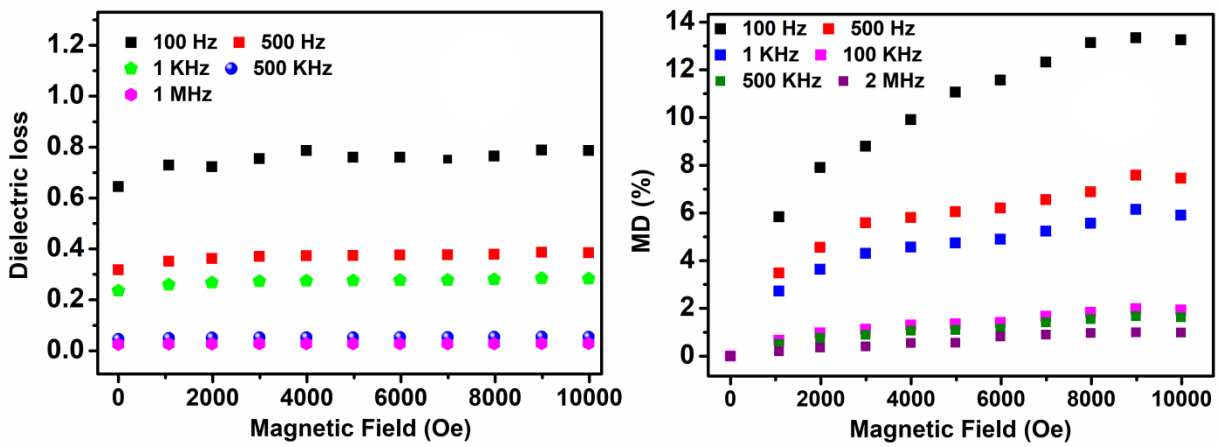

FIG 4. Room temperature magnetodielectric effect of Tb doped BFO NPs

Fig. 4 shows the room temperature magnetodielectric effect of Tb doped BFO NPs. Dielectric loss of the sample is almost unaffected with the application of external magnetic field. The enhancement in magneto-dielectric effect is clearly seen in the doped sample. When Tb doping concentration increases, the magneto dielectric effect rises. The magnetodielectric effect also rises with the intensity of applied magnetic field. The mismatch between the ionic radius of Bi atom with Tb ion produces magnetostriction effect with the application of magnetic field. It induces the electric field that helps in the ferroelectric domain alignment. This effectively enhances the magnetodielectric effect [19].

4. Conclusion

The effect of rare earth terbium doping on bismuth ferrite nanoparticles is discussed here. Terbium doping subsequently enhances electrical, dielectric, and magnetodielectric properties of the material. Morphological analysis also shows the uniform formation of nanoparticles with less agglomeration when doped with rare earth ion. The samples show non-Debye type dielectric relaxation behaviour.

5. Acknowledgements

The authors acknowledge DST-SERB (Grant No. EMR/2016/001409), DST-INSPIRE, Govt. of India, for financial support during this work.

REFERENCES

[1] V. V. Lazenka, M. Lorenz, H. Modarresi, K. Brachwitz, P. Schwinkendorf, T. Böntgen, J. Vanacken, M. Ziese, M. Grundmann, V. V. Moshchalkov, Journal of Physics D: Applied Physics, 2013, 46, 175006.
[2] M. K. Mishra, R. N. Mahaling, Ferroelectrics, 2017, 520(1), 184–195.
[3] S. M. Hossain, A. Mukherjee, S. Basu, M. Pal, Micro and Nano Letters, 2013, 8, 374-377.
[4] J. Wang, J. Hu, L. Yang, K. Zhu, B. W. Li, Q. Sun, Y. Li, J. Qiu. J Materiomics 4 (2018) 44.
[5] F. Zhang, X. Zeng, D. Bi, K. Guo, Y. Yao, S. Lu, Materials, 2018, 11**,** 2208.

[6] V. A. Khomchenko, D. A. Kiselev, E. K. Selezneva, J. M. Vieira, A. M. Lopes, Y. G. Pogorelov, J. P. Araujo, A. L. Kholkin, 2009, 321, 1692-1698.

[7] S. Chandel, P. Thakur, S. S. Thakur, V. Kanwar, M. Tomar, V. Gupta, A. Thakur, Ceramics International, 2018, 44(5), 4711-4718.

[8] P. Kumar, P. Chand, Journal of Alloys and Compounds, 2018, 748, 504-514.
[9] V. Singh, S. Sharma, R. K. Dwivedi, Journal of Alloys and Compounds," 2018, 747, 611-620.
[10] J. Zhu, J. Dai, J. Xu, X. Li, Ceramics International, 2018, 44, 9215-9220.
[11] A. Ghosh, D. P. Trujillo, H. Choi. S. M. Nakhmanson, S. P. Alpay, J. X. Zhu, Scientific Reports, 2019, 9, 194.
[12] F. Mumtaz, G. H. Jaffari, S. I. Shah, Journal of Physics: Condensed Matter, 2018, 30, 435802.
[13] M. Halder, A. K. Das, A. K. Meikap, Materials Research Bulletin, 2019, 104, 179–187.
[14] Rayssi, C., El.Kossi, S., Dhahri, J., & Khirouni, K. (2018). RSC Advances, 8(31), 17139–17150.
[15] F. Zhang, X. Zeng, D. Bi, K. Guo, Y. Yao, S. Lu, Materials, 2018, 11, 2208.
[16] A. Ashery, A. H. Zaki, M. H. Mourad, A. M. Azab, A. A. M. Farag, Bulletin of Materials Science, 2016, 39, 1057-1063.
[17] M. B. Hossen, A. K. M. A. Hossain, Journal of Advanced Ceramics, 2015, 4(3), 217–225.
[18] S. F. Chérif, A. Chérif, W. Dridi, M. F. Zid, Arabian Journal of Chemistry, 2020, 13, 5627-5638.
[19] A. Mukherjee, M. Banerjee, S. Basu, M. D. Mukadam, S. M. Yusuf, M. Pal, Materials Chemistry and Physics, 2015, 162, 140–148.